



Site-Selective Synthesis of Janus-type Metal-Organic Framework Composites**

Sudarat Yadnum, Jérôme Roche, Eric Lebraud, Philippe Négrier, Patrick Garrigue, Darren Bradshaw,* Chompunuch Warakulwit, Jumras Limtrakul, and Alexander Kuhn*

Abstract: Herein, bipolar electrochemistry is applied in a straightforward way to the site-selective *in situ* synthesis of metal–organic framework (MOF) structures, which have attracted tremendous interest in recent years because of their significant application potential, ranging from sensing to gas storage and catalysis. The novelty of the presented work is that the deposit can be intentionally confined to a defined area of a substrate without using masks or templates. The intrinsic site-selectivity of bipolar electrochemistry makes it a method of choice to generate, in a highly controlled way, hybrid particles that may have different functionalities combined on the same particle. The wireless nature of electrodeposition allows the potential for mass production of such Janus-type objects.

Microporous metal–organic frameworks (MOFs) assembled by coordination bonds between metal ions and organic ligands^[1] are of enormous importance for their applications in catalysis, gas separation, storage, drug delivery, and sensing.^[2] For MOFs to reach their full potential in these and other applications, it is necessary to process or directly prepare them in suitable application-specific configurations,^[3] such as

thin films and supported membranes,^[4] capsules,^[5] and composites.^[6] Often this involves MOF deposition, which is typically a bottom-up process, occurring preferentially at an appropriately functionalized surface^[7] obtained with a chemical or physical mask.^[8] Using these methods in combination with liquid-based epitaxy,^[9] reactive seeding,^[10] or electrochemistry,^[11] high-quality oriented MOF thin films and crystal arrays with micron-sized features have been prepared.^[8,12] Although significant progress has been made, challenges remain in the development of fast, inexpensive, and scalable fabrication processes, not only to facilitate MOF integration in real functional devices,^[13] but for the spatio-selective preparation of MOF-based structures. In particular, there are currently no satisfactory methods for the site-selective deposition of MOFs onto 3-dimensional substrates, thus forming Janus-type architectures; this is currently limited to MOF@MOF-type structures, where a close lattice match between the two frameworks is required for efficient epitaxial growth of one MOF crystal onto or around another.^[14] There are, however, significant benefits to developing such a strategy for MOF composites when one considers the strong concurrence between the inherent porosity and tuneable physical properties of MOFs with the applications of Janus structures in catalysis, drug delivery, optoelectronics, and biomedical imaging.^[15] Herein, we report for the first time the successful application of indirect bipolar electrodeposition (IBED)^[16] for the wireless and selective deposition of prototypical MOFs onto metallic wires and particles to prepare Janus-type composite materials in a facile manner under mild conditions.

Bipolar electrochemistry (BE) with micrometer-sized objects was first described by Fleischmann et al.^[17] When a conducting object is exposed to an electric field established between two electrodes in a solution, a positive and negative polarization occurs between the two opposite sides of the object where redox reactions can occur, if the polarization is strong enough.^[18] This concept has been explored in the context of various fields, including analytical chemistry,^[19] chemical motion,^[20] electronics,^[21] and materials science.^[22] Whereas BE is usually limited to deposits obtained from electroactive precursors,^[23] we have recently reported that insulating materials, including metal oxides and electrophoretic paints, can be generated from non-electroactive precursors.^[16] This IBED technique exploits an electrochemically triggered local pH change around the conducting objects, leading to controlled polymerization or precipitation of an insulating deposit, thus significantly extending the diversity of materials that can be prepared. The IBED approach is used in the present work to wirelessly generate reactive metal ions locally on the surface of metallic substrates that can

[*] S. Yadnum, Dr. J. Roche, P. Garrigue, Prof. A. Kuhn
Univ. Bordeaux, CNRS, ISM, UMR 5255, ENSCBP
33607 Pessac (France)
E-mail: kuhn@enscbp.fr
Homepage: <http://www.enscbp.fr/nsysa/home.asp>

S. Yadnum, Dr. C. Warakulwit, Prof. J. Limtrakul
Department of Chemistry, Faculty of Science, Kasetsart University
Bangkok 10900 (Thailand)


Prof. J. Limtrakul
PTT Group Frontier Research Center, PTT Public Company Limited
555 Vibhavadi Rangsit Road, Chatuchak, Bangkok 10900 (Thailand)

Dr. D. Bradshaw
School of Chemistry, University of Southampton
Highfield, Southampton, SO17 1BJ (UK)
E-mail: D.Bradshaw@soton.ac.uk

E. Lebraud
CNRS, Univ. Bordeaux, ICMCB, UPR 9048
33600 Pessac (France)

P. Négrier
Laboratoire Ondes et Matière d'Aquitaine, CNRS UMR 5798
33405 Talence (France)

[**] The Thailand Research Fund (TRF) is acknowledged for a Royal Golden Jubilee Ph.D. Fellowship (3.C.KU/51/A.1) and the French Government for its contribution to this Ph.D. co-tutelle program. D.B. thanks the European Research Council (ERC) for financial support (BIOMOF-258613). A.K. acknowledges support from the Institut Universitaire de France ANR project EMMA 00701.

 Supporting information for this article is available on the WWW under <http://dx.doi.org/10.1002/anie.201400581>.

subsequently react with ligand species in solution to form extended coordination-based network structures. Although MOFs have previously been electrochemically prepared by anodic dissolution^[24] and cathodic electroreduction of base equivalents for ligand deprotonation,^[25] IBED is qualitatively distinct, as it permits wireless selective deposition of MOFs at one end or hemisphere of a substrate where polarization simultaneously generates the metal ions required for framework growth and acts as a simple virtual mask without the need to chemically or physically block areas where deposition is not desired.

To demonstrate the application of IBED to MOFs, we initially selected the chemically and thermally stable tetrahedrally coordinated Zn–imidazolate network [Zn(2-MeIm)₂] ZIF-8 (2-MeIm = 2-methylimidazole),^[26] due to its reliable synthesis in a range of solvents under mild conditions.^[27] We employed a metallic Zn wire as both a metal source and substrate for selective deposition. To carry out these reactions, one has to consider that in BE the polarization voltage generated between the two sides of an object with respect to the surrounding solution is proportional to the external electric field (E) and the length of the object (l):

$$\Delta V = E \times l \quad (1)$$

In a first-order approximation, ΔV must be at least equal to the difference between the formal potentials of the two involved redox couples. In the present case, oxidation of Zn metal occurs at the positively polarized side of a zinc wire (Figure 1a), based on the following redox couple:

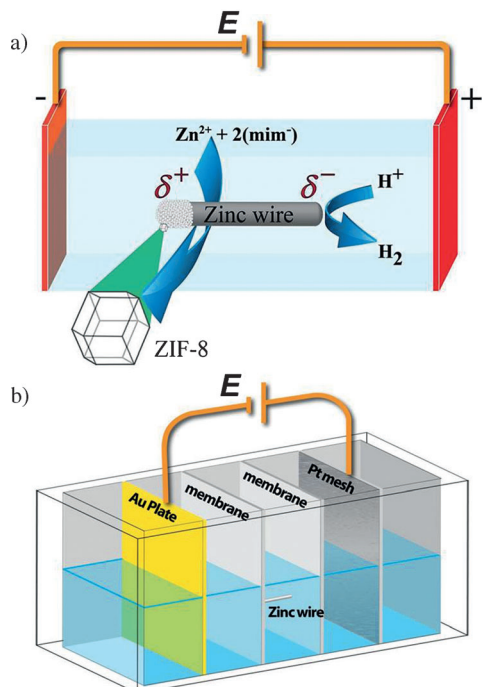
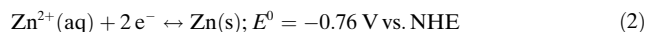


Figure 1. a) Mechanism of the formation of ZIF-8. Crystal growth on the anodically polarized side of a zinc wire is triggered by indirect bipolar electrodeposition (IBED). b) Design of the bipolar electrochemical cell used for the synthesis of ZIF-8.



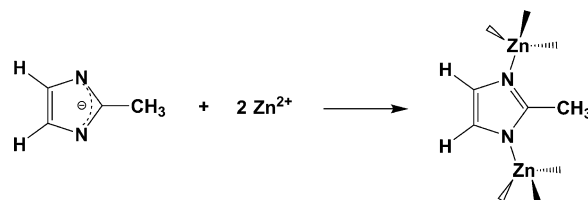
At the opposite side of the wire, protons are simultaneously reduced:



such that, under standard conditions, the combination of these two redox couples leads, from a thermodynamic point of view, to a spontaneous reaction between both redox couples. However, variable overpotentials from potential drops at the electrodes and in the solution, as well as slow kinetics, also need to be considered, and especially changes in pH will equally impact the potential difference. To experimentally estimate the potential difference required to drive the two redox reactions simultaneously at both ends of the wire with sufficiently high kinetics, cyclic voltammetry has been used (Figure S11).

The electrochemical cell for ZIF-8 synthesis was composed of two electrodes, and a 1 cm Zn wire was placed at the center between two Nafion membranes that are present to avoid parasitic reactions of the ligand at the feeder electrodes (Figure 1b). The two electrodes are separated by 3.5 cm, and when applying a potential difference of 5 V between them, one can calculate (based on [Eq. 1]), that a potential drop of 1.4 V should occur between the two ends of the Zn wire; according to the CV shown in Figure S11 in the Supporting Information, this is sufficient to overcome possible overpotentials and induce the required redox reactions at the opposite ends of the wire.

The Zn^{2+} ions produced at the positively polarized side of the wire undergo a chemical reaction with the 2-MeIm linker group (Scheme 1). In a control experiment where a Zn wire



Scheme 1. Reaction of the 2-methylimidazole linker with Zn^{2+} ions at the surface of a bipolar electrode to form the basic building unit of ZIF-8 crystals.

was left in an aqueous solution of the ligand for three days without applying a potential (Figure 2a), almost no spontaneous reaction occurs, with only a few small deposits located at random positions along the wire. However, when applying the electric field, ZIF-8 is generated as a crystalline deposit exclusively at the positively polarized end of the wire (Figure 2b).

The SEM images of the IBED-synthesized ZIF-8 samples using different potentials, electrodeposition times, and concentrations of 2-MeIm are shown in Figure 2. In contrast to previous reports where no ZIF-8 deposition occurred onto “wired” Zn anodes,^[24b] we clearly observe the formation of surface bound ZIF-8 crystals. As a consequence of the

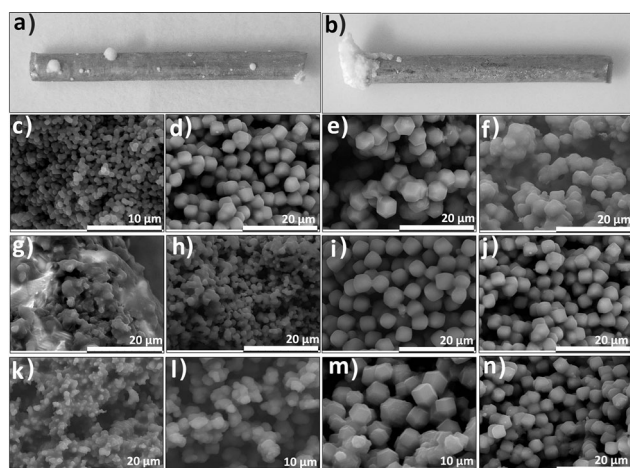


Figure 2. Site-selective modification of a zinc wire with ZIF-8: a) Control experiment without electric field after three days in a solution containing 2-Melm (1.376 M) and Na_2SO_4 (0.05 M). b) Synthesized by the IBED method (6 V, 60 min, 1.376 M 2-Melm, 0.05 M Na_2SO_4). c–n) SEM images of ZIF-8, as-synthesized by IBED. c–f) Crystals obtained for different external potential differences with 2-Melm (1.376 M) after 60 min reaction time: c) 5 V, d) 6 V, e) 7 V, and f) 8 V. g–j) Deposits observed for different electrodeposition times with 2-Melm (1.376 M) and 6 V between the external feeder electrodes: g) 2 min, h) 10 min, i) 30 min, and j) 60 min. k–n) Morphology of the obtained crystals for different concentrations of 2-Melm after 60 min electrodeposition time at 6 V: k) 0.344 M, l) 0.688 M, m) 1.032 M, and n) 1.376 M.

polarization of the substrate, deposition continues at one end of the wire with increasing reaction time (Figure 2b), rather than leading to even coverage, as observed with conventional electrochemical systems.^[24b] This strongly suggests that the electrochemically generated Zn^{2+} ions can migrate through the porous ZIF-8 deposit and/or interstices between crystals to continue to induce growth at its outer surface. Eventually, linker could also diffuse through the deposit towards the inner interface between zinc and the MOF,^[28] but in a less efficient way than the positively charged zinc ions attracted by the feeder cathode.

For the optimized synthesis parameters of 6 V of external potential applied for 60 min (Figure 2d,j,n), the obtained ZIF-8 is composed of crystals with a rhombic dodecahedral morphology and uniform size (ca. 4 μm), which matches well with the reported morphology for this zeotype extended network.^[27b] For IBED MOF generation, the external electric field applied during synthesis plays an important role with respect to the crystal size and morphology of the generated ZIF-8, under otherwise identical conditions. As shown in Figure 2c–e, the crystal size increases when increasing the potential difference, at constant 2-Melm concentration. In all cases, rhombic dodecahedral crystals are formed, and the observed size increase is consistent with a decrease in the 2-Melm/ Zn^{2+} ratio, as reported for bulk ZIF-8 synthesis in water.^[29] However, crystal morphology becomes less well-defined at too high potentials. At 8 V (Figure 2f) for example, the particles appear fused together, possibly as a result of co-deposition of impurity phases, arising from the low 2-Melm/ Zn^{2+} ratio,^[29] owing to the relatively rapid release of Zn^{2+} at

this potential. For such a relative deficiency of ligand, the formed zinc ions are more likely to form zinc hydroxides (Figures S1, S2, and S4). This strongly suggests that a close match between the release rate of metal ions (which is readily controlled by the applied potential), MOF nucleation, and growth kinetics is required to form well-defined crystals.

Electrodeposition time also affects the amount and morphology of the product (Figure 2g–j), and as expected, the amount of product and crystal size increases and morphology becomes better defined with increasing reaction time. Recent reports based on studies performed in situ on early-stage ZIF-8 growth using SAXS^[30] and time-resolved static light-scattering^[31] indicate that nucleation is a slow continuous process, whereas crystal growth is more rapid. However the growth mechanism of coordination-based materials under the synthesis conditions present around bipolar electrodes is complex,^[32] and local effects such as pH and concentration gradients certainly play an important role.

Figure 2k–n show SEM images of ZIF-8 prepared with different concentrations of 2-Melm, keeping the electrodeposition time and the applied electric field constant at 60 min and 6 V, respectively. Increasing the 2-Melm/ Zn^{2+} molar ratio also improves the crystal morphology and highly faceted crystals are obtained at the highest concentrations of 2-Melm. Under these conditions, all the Zn^{2+} ions produced react with the organic linker, and the excess 2-Melm could potentially act to stabilize and/or control ZIF-8 crystal growth.^[31] At lower 2-Melm concentrations however, the Zn wire is still oxidized at the same rate, but insufficient linker is available to lock all of the metal ions into the extended ZIF structure, thus leading to the formation of other Zn-containing species, including oxides and/or hydroxides, as previously observed for the aqueous synthesis of bulk ZIF-8 at low 2-Melm/ Zn ratios.^[29] This is an analogous situation to using high potentials, as shown in Figure 2f (see also Figures S1, S2, and S4).

The ZIF-8 crystals obtained by IBED were characterized by powder X-ray diffraction (PXRD) (Figure 3) and infrared (IR) spectroscopy (see the Supporting Information). Figure 3 shows diffraction peak positions and relative diffraction intensities of ZIF-8 products recorded from three samples obtained from solutions containing different concentrations of 2-Melm after applying a potential of 6 V for 60 min. The products prepared at high concentrations of 2-Melm were assigned to sodalite (SOD) network-type structures and a typical reflection pattern for the synthesized ZIF-8 corresponding to the (011), (002), (112), (022), (013), and (222) planes was observed, which is in excellent agreement with those described in the literature.^[33]

Control experiments that were carried out with a zinc wire attached and electrically connected to the working electrode in a normal three-electrode setup only resulted in homogeneous coverage of the wire with the MOF, but never in a site-selective deposition (see the Supporting Information). This clearly demonstrates that the proposed approach is unique in terms of the formation of these Janus-type objects.

To illustrate the general validity of the IBED concept for site-selective MOF deposition, we also investigated the

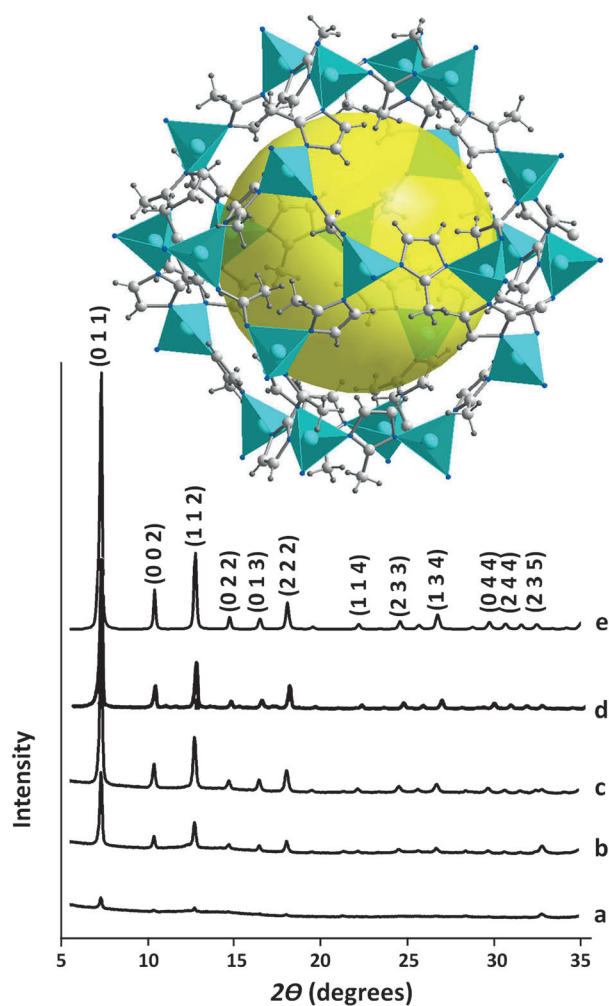


Figure 3. Structure of the ZIF-8 sodalite cage refined from the powder data of IBED deposited material (top). PXRD patterns illustrating the structural evolution of ZIF-8 obtained by IBED when applying an electric field of 6 Volts for 60 min as a function of the concentration of 2-methylimidazole: a) 0.688 M, b) 1.032 M, c) 1.376 M, d) XRD pattern of ZIF-8 from literature,^[33] and e) Simulated XRD pattern of ZIF-8 powder.

formation of HKUST-1,^[34] a commercially important microporous framework $[\text{Cu}_3(\text{BTC})_2(\text{H}_2\text{O})_3]$ (BTC = 1,3,5-benzenetricarboxylate). HKUST-1 has previously been prepared electrochemically through anodic dissolution of wired Cu electrodes^[24] and selectively deposited onto printed circuit boards.^[11] In the current work, an isotropic Cu metal bead was employed as the substrate where the wireless oxidation of copper in ethanol (Figure 4b) produces the Cu^{2+} ions necessary for the local formation of the MOF on one hemisphere only, leading to a well-defined Janus-type composite particle. The position and extension of the blue crystalline MOF deposit can be readily controlled by the applied external voltage owing to the change of polarization (Figure 4c,d). When the material deposited on the anodic side of this Janus object is characterized by SEM, the familiar octahedral block-like crystals of HKUST-1 are observed, further confirming the successful generation of the MOF (see the Supporting Information) under these conditions. As the

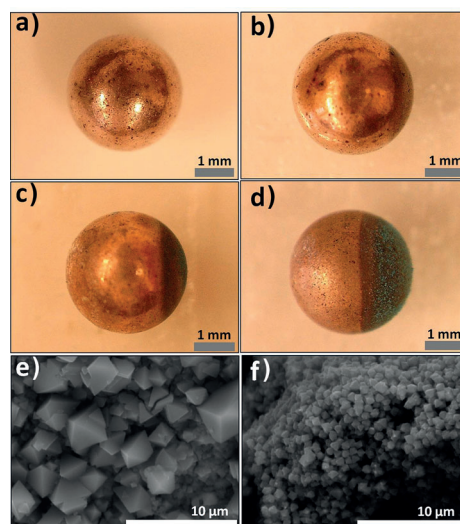


Figure 4. Site-selective modification of a copper bead (3 mm diameter) with HKUST-1: a) bead before modification, b) after applying an external potential difference of 10 Volts for 60 min without 1,3,5-benzenetricarboxylic acid, and c,d) bead obtained at 10 V and 20 V, respectively, in the presence of 1,3,5-benzenetricarboxylic acid (0.08 M) in ethanol after 60 min reaction time. e,f) SEM images of HKUST-1 as-synthesized by IBED on one side of the copper bead; crystals obtained at 10 V and 20 V, respectively, in 1,3,5-benzenetricarboxylic acid (0.08 M) after 60 min reaction time.

applied potential increases from 10 V to 20 V, the crystal size decreases in agreement with previous studies on the electrochemical deposition of HKUST-1.^[11] The deposit has been further characterized using XRD and FTIR spectroscopy (Figures S3 and S10). Control experiments exposing the copper bead to the ligand solution without applying an electric field did not result in the formation of HKUST-1, even after three days (see the Supporting Information). Furthermore, attaching the bead to the working electrode of a three-electrode setup leads to a homogeneous and complete MOF coverage (see the Supporting Information), which indicates that the bipolar setup is absolutely crucial to produce the asymmetric composite particles.

In summary, we report here for the first time the straightforward and site-selective synthesis of MOF compounds by indirect bipolar electrochemistry with two representative proof-of-principle experiments for the asymmetric generation of MOFs on the surface of isotropic and anisotropic substrates. The characterization of the obtained compounds confirms their successful synthesis, where crystal size and morphology can be tuned in a facile manner through modulation of linker concentration, electrodeposition time, and the magnitude of the external electric field. This concept might be generalized for the synthesis of many other MOF compounds, thus allowing inexpensive and green access to this important family of microporous materials, and leading to a new generation of MOF-based Janus-type composites with applications in catalysis, separation, storage, and sensing.

Received: January 20, 2014

Published online: March 6, 2014

Keywords: composites · electrochemistry · electrocrystallization · Janus particles · metal-organic frameworks

- [1] a) S. Kitagawa, R. Kitaura, S.-I. Noro, *Angew. Chem.* **2004**, *116*, 2388–2430; *Angew. Chem. Int. Ed.* **2004**, *43*, 2334–2375; b) G. Férey, *Chem. Soc. Rev.* **2008**, *37*, 191–214; c) C. Janiak, J. K. Vieth, *New J. Chem.* **2010**, *34*, 2366–2388.
- [2] J. R. Long, O. M. Yaghi, *Chem. Soc. Rev.* **2009**, *38*, 1213–1214.
- [3] D. Bradshaw, A. Garai, J. Huo, *Chem. Soc. Rev.* **2012**, *41*, 2344–2381.
- [4] O. Shekhah, J. Liu, R. A. Fischer, C. Woll, *Chem. Soc. Rev.* **2011**, *40*, 1081–1106.
- [5] R. Ameloot, F. Vermoortele, W. Vanhove, M. B. J. Roeffaers, B. F. Sels, D. E. De Vos, *Nat. Chem.* **2011**, *3*, 382–387.
- [6] A. Ahmed, M. Forster, R. Clowes, D. Bradshaw, P. Myers, H. Zhang, *J. Mater. Chem. A* **2013**, *1*, 3276–3286.
- [7] D. Zacher, O. Shekhah, C. Woll, R. A. Fischer, *Chem. Soc. Rev.* **2009**, *38*, 1418–1429.
- [8] P. Falcaro, D. Buso, A. J. Hill, C. M. Doherty, *Adv. Mater.* **2012**, *24*, 3153–3168.
- [9] O. Shekhah, H. Wang, S. Kowarik, F. Schreiber, M. Paulus, M. Tolan, C. Sternemann, F. Evers, D. Zacher, R. A. Fischer, C. Wöll, *J. Am. Chem. Soc.* **2007**, *129*, 15118–15119.
- [10] Y. Hu, X. Dong, J. Nan, W. Jin, X. Ren, N. Xu, Y. M. Lee, *Chem. Commun.* **2011**, *47*, 737–739.
- [11] R. Ameloot, L. Stappers, J. Franssaer, L. Alaerts, B. F. Sels, D. E. De Vos, *Chem. Mater.* **2009**, *21*, 2580–2582.
- [12] A. Bétard, R. A. Fischer, *Chem. Rev.* **2012**, *112*, 1055–1083.
- [13] M. D. Allendorf, A. Schwartzberg, V. Stavila, A. A. Talin, *Chem. Eur. J.* **2011**, *17*, 11372–11388.
- [14] S. Furukawa, K. Hirai, K. Nakagawa, Y. Takashima, R. Matsuda, T. Tsuruoka, M. Kondo, R. Haruki, D. Tanaka, H. Sakamoto, S. Shimomura, O. Sakata, S. Kitagawa, *Angew. Chem.* **2009**, *121*, 1798–1802; *Angew. Chem. Int. Ed.* **2009**, *48*, 1766–1770.
- [15] *Janus Particle Synthesis Self-Assembly and Applications* (Eds.: S. Jiang, S. Granick), The Royal Society of Chemistry, London, **2012**.
- [16] G. Loget, J. Roche, E. Gianessi, L. Bouffier, A. Kuhn, *J. Am. Chem. Soc.* **2012**, *134*, 20033–20036.
- [17] M. Fleischmann, J. Ghoroghchian, D. Rolison, S. Pons, *J. Phys. Chem.* **1986**, *90*, 6392–6400.
- [18] a) G. Loget, A. Kuhn, *Anal. Bioanal. Chem.* **2011**, *400*, 1691–1704; b) F. Mavré, R. K. Anand, D. R. Laws, K.-F. Chow, B.-Y. Chang, J. A. Crooks, R. M. Crooks, *Anal. Chem.* **2010**, *82*, 8766–8774.
- [19] a) S. E. Fosdick, K. N. Knust, K. Scida, R. M. Crooks, *Angew. Chem. Int. Ed.* **2013**, *52*, 10438–10456; b) J. P. Guerrette, S. M. Oja, B. Zhang, *Anal. Chem.* **2012**, *84*, 1609–1616; c) J. P. Guerrette, S. J. Percival, B. Zhang, *J. Am. Chem. Soc.* **2013**, *135*, 855–861.
- [20] a) G. Loget, A. Kuhn, *J. Am. Chem. Soc.* **2010**, *132*, 15918–15919; b) G. Loget, A. Kuhn, *Lab Chip* **2012**, *12*, 1967–1971; c) G. Loget, A. Kuhn, *Nat. Commun.* **2011**, *2*, 535.
- [21] J.-C. Bradley, H.-M. Chen, J. Crawford, J. Eckert, K. Ernazarova, T. Kurzeja, M. Lin, M. McGee, W. Nadler, S. G. Stephens, *Nature* **1997**, *389*, 268–271.
- [22] a) C. Ulrich, O. Andersson, L. Nyholm, F. Björefors, *Angew. Chem.* **2008**, *120*, 3076–3078; *Angew. Chem. Int. Ed.* **2008**, *47*, 3034–3036; b) S. Ramakrishnan, C. Shannon, *Langmuir* **2010**, *26*, 4602–4606; c) Y. Ishiguro, S. Inagi, T. Fuchigami, *Langmuir* **2011**, *27*, 7158–7162; d) J.-C. Bradley, S. Babu, A. Mittal, P. Ndungu, B. Carroll, B. Samuel, *J. Electrochem. Soc.* **2001**, *148*, C647–C651; e) J. C. Bradley, S. Babu, P. Ndungu, *Fullerenes Nanotubes Carbon Nanostruct.* **2005**, *13*, 227–237; f) S. Babu, P. Ndungu, J.-C. Bradley, M. Rossi, Y. Gogotsi, *Microfluid. Nanofluid.* **2005**, *1*, 284–288; g) G. Loget, D. Zigah, L. Bouffier, N. Sojic, A. Kuhn, *Acc. Chem. Res.* **2013**, *46*, 2513–2523.
- [23] G. Loget, V. Lapeyre, P. Garrigue, C. Warakulwit, J. Limtrakul, M.-H. Delville, A. Kuhn, *Chem. Mater.* **2011**, *23*, 2595–2599.
- [24] a) U. Mueller, M. Schubert, F. Teich, H. Puetter, K. Schierle-Arndt, J. Pastre, *J. Mater. Chem.* **2006**, *16*, 626–636; b) A. M. Joaristi, J. Juan-Alcaniz, P. Serra-Crespo, F. Kapteijn, J. Gascon, *Cryst. Growth Des.* **2012**, *12*, 3489–3498.
- [25] M. Li, M. Dincă, *J. Am. Chem. Soc.* **2011**, *133*, 12926–12929.
- [26] K. S. Park, Z. Ni, A. P. Côté, J. Y. Choi, R. Huang, F. J. Uribe-Romo, H. K. Chae, M. O’Keeffe, O. M. Yaghi, *Proc. Natl. Acad. Sci. USA* **2006**, *103*, 10186–10191.
- [27] a) Y. Pan, Y. Liu, G. Zeng, L. Zhao, Z. Lai, *Chem. Commun.* **2011**, *47*, 2071–2073; b) J. Cravillon, S. Münzer, S.-J. Lohmeier, A. Feldhoff, K. Huber, M. Wiebcke, *Chem. Mater.* **2009**, *21*, 1410–1412.
- [28] M. Li, M. Dincă, *Chem. Sci.* **2014**, *5*, 107–111.
- [29] K. Kida, M. Okita, K. Fujita, S. Tanaka, Y. Miyake, *CrystEngComm* **2013**, *15*, 1794–1801.
- [30] J. Cravillon, C. A. Schröder, R. Nayuk, J. Gummel, K. Huber, M. Wiebcke, *Angew. Chem.* **2011**, *123*, 8217–8221; *Angew. Chem. Int. Ed.* **2011**, *50*, 8067–8071.
- [31] J. Cravillon, R. Nayuk, S. Springer, A. Feldhoff, K. Huber, M. Wiebcke, *Chem. Mater.* **2011**, *23*, 2130–2141.
- [32] Z. Fattah, J. Roche, P. Garrigue, D. Zigah, L. Bouffier, A. Kuhn, *ChemPhysChem* **2013**, *14*, 2089–2093.
- [33] S. R. Venna, J. B. Jasinski, M. A. Carreon, *J. Am. Chem. Soc.* **2010**, *132*, 18030–18033.
- [34] S. S.-Y. Chui, S. M.-F. Lo, J. P. H. Charmant, A. G. Orpen, I. D. Williams, *Science* **1999**, *283*, 1148–1150.